

## Full Paper

## 2-Benzamido-4-methylthiazole-5-carboxylic Acid Derivatives as Potential Xanthine Oxidase Inhibitors and Free Radical Scavengers

Md. Rahmat Ali<sup>1</sup>, Suresh Kumar<sup>1</sup>, Obaid Afzal<sup>1</sup>, Nishtha Shalmali<sup>1</sup>, Wazid Ali<sup>2</sup>, Manju Sharma<sup>3</sup>, and Sandhya Bawa<sup>1</sup>

<sup>1</sup> Faculty of Pharmacy, Department of Pharmaceutical Chemistry, Hamdard University, New Delhi, India

<sup>2</sup> Hamdard Institute of Medical Science, Hamdard University, New Delhi, India

<sup>3</sup> Faculty of Pharmacy, Department of Pharmacology, Hamdard University, New Delhi, India

The new chemical entities febuxostat and topiroxostat have been approved by the US Food and Drug Administration, opening new avenues for exploiting different heterocycles other than purines as xanthine oxidase (XO) inhibitors. A different series of substituted 2-benzamido-4-methylthiazole-5-carboxylic acid derivatives (**5a–r**) was synthesized and characterized by the collective use of IR, <sup>1</sup>H and <sup>13</sup>C NMR, and mass spectroscopy, for the treatment of gout and hyperuricemia. *In vitro* studies of the synthesized derivatives revealed that the presence of a fluoro group at the *para* position in **5b** (IC<sub>50</sub> = 0.57 μm) and a chloro group in **5c** (IC<sub>50</sub> = 0.91 μm) signifies excellent XO inhibitory activity among the series, along with their DPPH free radical scavenging activity. *In vivo* serum uric acid inhibition studies established that **5b** and **5c** displayed 62 and 53% uric acid inhibition, respectively. Studies on enzyme kinetics indicated that **5b** acts as a mixed type inhibitor. *In silico* prediction by various softwares also helped in the recognition of potent XO inhibitors.

**Keywords:** Febuxostat / Kinetic / Reactive oxygen species / Uric acid / Xanthine oxidase

Received: October 25, 2016; Revised: January 1, 2017; Accepted: January 4, 2017

DOI 10.1002/ardp.201600313

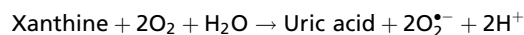


Additional supporting information may be found in the online version of this article at the publisher's web-site.

### Introduction

Gout is a common metabolic disorder, which is usually associated with repeated incidences of pain, inflammation, etc. Such a condition generally originates due to increases in the deposition of monosodium urate (MSU) crystals in articular and periarticular tissues, which further generates characteristic intermittent chronic cartilage injury and acute inflammation of the gouty joint [1–3]. Uric acid is the final metabolite of purine degradation pathway in the human body and is eventually excreted by the kidneys and to a lesser

extent through the gastrointestinal tract. Conclusively, the excessive production of uric acid or impaired renal excretion of uric acid are the main causes of gout and the associated symptoms [4, 5]. Xanthine oxidase (XO, E.C. 1.1.3.22) is a complex metalloflavoprotein in the purine scavenging pathway which activates the transformation of hypoxanthine to xanthine and xanthine to uric acid [6]. The oxygen molecules act as electron acceptor through re-oxidation advancement of OX which produces superoxide radicals and hydrogen peroxide [7]. These biochemical reactions can be represented as follows [8]:



Therefore, xanthine oxidase acts as important biological source of superoxide radicals, which imparts oxidative stress effect on human beings. These reactive oxygen species (ROS)

**Correspondence:** Dr. Sandhya Bawa, Faculty of Pharmacy, Department of Pharmaceutical Chemistry, Jamia Hamdard (Hamdard University), New Delhi 110062, India.  
**E-mail:** drsbawa@rediffmail.com, sbawa@jamiahamdard.ac.in  
**Fax:** +91 11 26059663

are entangled with several pathological conditions such as aging, atherosclerosis, inflammation, cancer, etc. [9]. Along with this, they are also involved in the development of ischemia-reperfusion injury, various cardiovascular and inflammatory diseases [10–13]. The nitric oxide signaling pathway and production of ROS together increase vascular oxidative stress in patients with chronic heart failure and are also involved in development of cardiomyopathy in type I diabetes, which is closely associated with increased activity of endothelium bound xanthine oxidase [14–16]. Hence the regulation of xanthine oxidase activity in human body is very much needed for the anticipation of several diseases and human health.

Keeping in view the above facts, the use of XO inhibitors should be regarded as an imperative therapeutic approach for the treatment of gout and associated complications. Oxypurinol (2), a metabolite of allopurinol (1), is a renowned purine analog and XO inhibitor and has been widely used in treatment of gout for many years [17–19]. However, severe life-threatening side effects have been reported in some cases which include a toxicity syndrome executed by vasculitis, eosinophilia, rash hepatitis, and progressive renal failure due to purine backbone of allopurinol and its analogs [20, 21]. Therefore, there is an immense need of evolving non-purine alternatives to allopurinol with potent XO inhibitory activity and better safety profile. In 2009, the US Food and Drug Administration (US FDA) approved febuxostat (3), a thiazole derivative and non-purine XO inhibitor which attracted worldwide attention [22, 23]. A recent drug topiroxostat (4) has been

launched in Japan in the year 2013. This derivative is approved for the treatment of gout and hyperuricemia [24, 25]. Reduction in uric acid levels may also be achieved by using uricosuric agents. A latest example is lesinurad (11) that increases the urinary excretion of uric acid by interfering with the urate absorption from kidney to blood [26].

Higher incidences of toxic effects were observed during clinical study of above-described drugs and these effects were also associated with large amount of superoxide anion generation by XO involved in the various pathological conditions. Therefore, development of XO inhibitors with free radical scavenging potential may prove as promising agents to treat gout. These possibilities have encouraged the researchers to develop structurally diverse molecules lacking of purine backbone with promising XO inhibitory activity. The replacement of thiazole with other heterocyclic rings further leads to febuxostat analogs having carboxyl ring in their structures. Some examples are 4-methyl-2-((2-methylbenzyl)amino)thiazole-5-carboxylic acid (5), Y-700 (6), selenazoles (7), isoxazoles (8), oxazole (9), pyridines (10), 2-(indol-5-yl)thiazoles (11), and imidazole's (13) derivatives (Fig. 1) [27–32]. It was assumed worthy to design structural analogs of febuxostat rationally as non-purine XO inhibitors with antioxidant activity and reduced associated toxicities. In continuation of our earlier efforts on finding novel non-purine XO inhibitors (5), we have designed, synthesized, and evaluated 2-benzamido-4-methylthiazole-5-carboxylic acid derivatives (5a–r) (Fig. 2) as potent XO inhibitors and free radical scavengers.

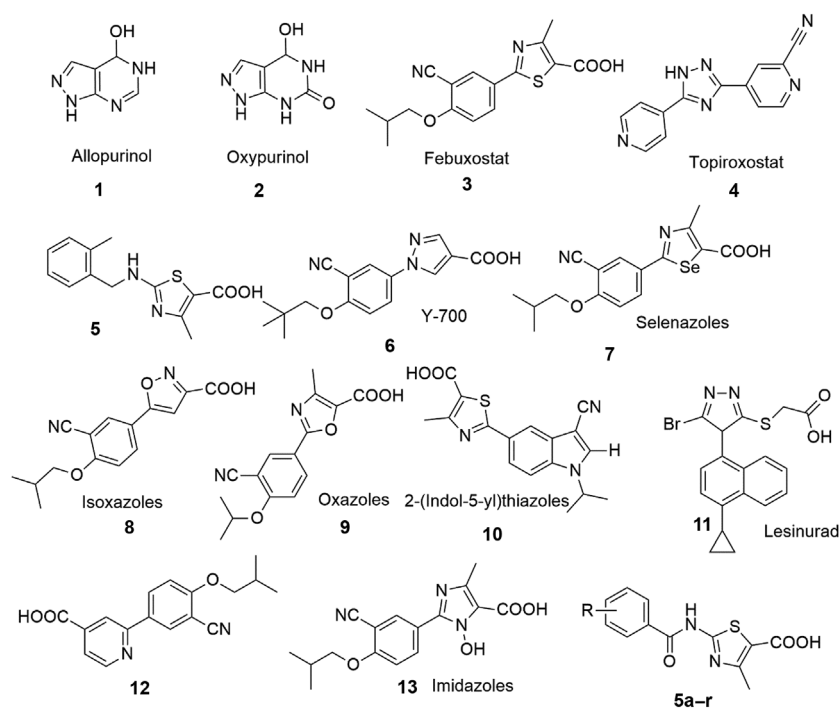


**Figure 1.** Chemical structures of various inhibitors of xanthine oxidase and its analogs. Allopurinol, febuxostat, and topiroxostat are FDA-approved drugs for the treatment of gout. Oxypurinol (alloxanthine) is the hydroxylation product of allopurinol by XO and inhibits XO via direct coordination of its N<sub>2</sub> atom to Mo of the enzyme active site. Replaced thiazole with other heterocyclic rings, including carboxyl moiety containing inhibitors. Lesinurad a recently approved drug for the use of urate lowering therapy. Newly designed compounds (5a–r) as XO inhibitors.

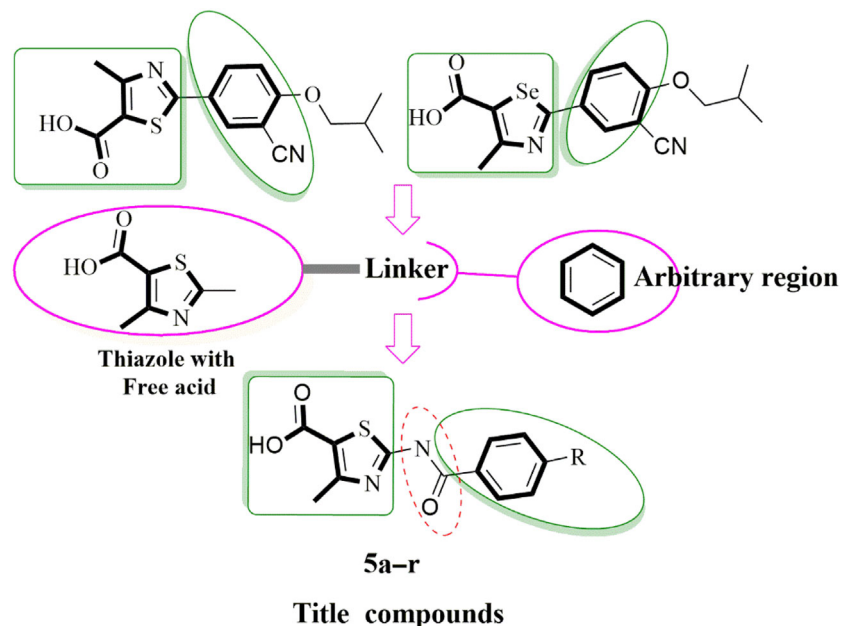


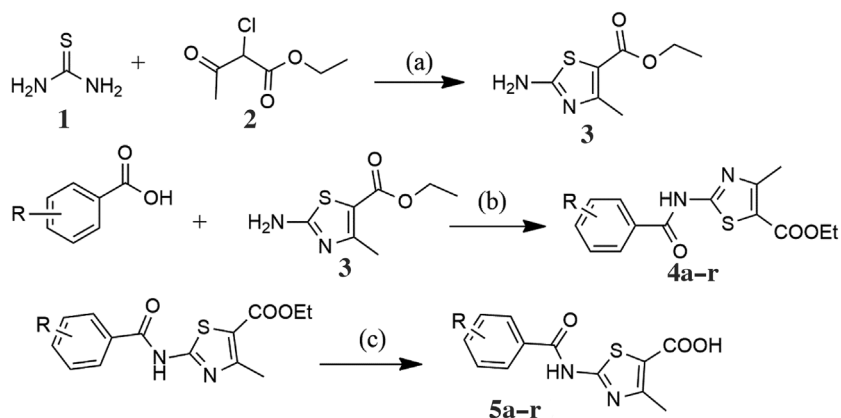
**Figure 2.** Chemical architecture of febuxostat and its analog for development of 2-benzamido-4-methylthiazole-5-carboxylic acid derivatives (**5a-r**) as XO inhibitors and free radical scavengers.

## Result and discussion

### Chemistry

2-Benzamido-4-methylthiazole-5-carboxylic acid derivatives as XO inhibitors (**5a-r**) were synthesized as outlined in Scheme 1. Thiourea and commercially available 2-chloroethylacetate was cyclized to form ethyl 2-amino-4-methyl-1,3-thiazole-5-carboxylate ester (**3**) [33–35]. Subsequently, reaction was carried out by stirring equivalent amounts of substituted aromatic acid and ethyl 2-amino-4-methyl-1,3-thiazole-5-carboxylate ester in dry pyridine. *In situ* formation of amide at 0–5°C temperature was

achieved by adding  $\text{POCl}_3$  dropwise as condensing agent. An acylating agent was first generated *in situ* after the addition of acid which then reacted with the added amine and finally led to an amide. The acid here acted as an activating or coupling agent. This one-pot procedure involved the formation of acylating agents along with the amide at 0–5°C temperature [36]. The substituted benzamide esters (**4a-r**) were hydrolyzed with potassium carbonate to get substituted 2-benzamido-4-methylthiazole-5-carboxylic acid derivatives (**5a-r**) (after acidification) as target compounds [33]. All synthesized compounds were characterized by collective use of IR,  $^1\text{H}$  and  $^{13}\text{C}$  NMR, and mass



R = H, 4-F, 4-Cl, 4-Br, 4-CH<sub>3</sub>, 4-OH, 4-OCH<sub>3</sub>, 4-NO<sub>2</sub>, 2-F, 2-Cl, 2-Br, 2-CH<sub>3</sub>, 2-NO<sub>2</sub>, 2-OCH<sub>3</sub>, 2-OH, 3-Cl, 4-F, 3-Cl, 3-Br.

**Scheme 1.** Route of synthesis of 2-(benzylamino)-4-methyl-1,3-thiazole-5-carboxylic acid derivatives (**5a-r**). Reagents and conditions: (a) Ethanol, reflux, 70°C; (b) dry pyridine,  $\text{POCl}_3$ , stirring, RT; (c)  $\text{K}_2\text{CO}_3$ , stirring with reflux.

spectroscopy. All spectral values were in accordance with the assumed structures. IR spectral data characterized the presence of carbonyl function of carboxylic acid which appeared as stretching band at  $1665\text{ cm}^{-1}$ , and carbonyl function of amide appeared as stretching band at  $1742\text{ cm}^{-1}$ . N–H stretching band appeared at  $3243\text{ cm}^{-1}$ , C–N stretching at  $1202\text{ cm}^{-1}$  for compound **5a**, the OH stretching band of carboxyl appeared at  $3063\text{ cm}^{-1}$ . In  $^1\text{H}$  NMR spectral analysis of compound **4a**, the ester proton resonated as a doublet and quartet at  $\delta$  1.25 and 4.37 ppm, which disappeared in spectrum of compound **5a**, and a new peak of carboxylic acid was observed at high downfield values at  $\delta$  10.52 ppm (bs, 1H) integrating for one proton. The signal due to –CONH– proton was also observed at high downfield  $\delta$  12.22 ppm ( $\text{D}_2\text{O}$  exchangeable). The methyl group of thiazole ring appeared as singlet at  $\delta$  2.26 ppm and the aromatic proton appeared as multiplet at  $\delta$  6.82–7.86 ppm of compound **5a**. Furthermore, in  $^{13}\text{C}$  NMR spectrum of the compound **5a**, signal due to the carbonyl carbon of amide was observed at  $\delta$  163.54 ppm (CONH), and carbonyl carbon of carboxylic acid was observed at  $\delta$  167.70 ppm (CO), respectively. Also a thiazole carbon signal was found in the  $^{13}\text{C}$  NMR spectrum of compounds **5a** at 145.86, 156.54, and 158.70, ppm. The molecular ion peak of compound **5a** appeared at  $m/z$  263.01 (M + H) in mass spectrum. The elucidation of spectral data and elemental analysis showed successful synthesis of desired compounds. The specific spectral details of synthesized compounds (**5a–r**) with their structural characterization data are mentioned in the Experimental section.

## In silico computational studies

### Physicochemical properties

For the design and development of XO inhibitors with enriched pharmacological profile, the prediction of physicochemical properties is most important. Improved lipophilicity with poor water solubility is one of these significant parameters. The drug-likeness characters such as lipophilicity (clogP), water-solubility (clogS), molecular weight (MW), number of rotatable bonds (NROTB), and drug-likeness grade of Lipinski's rule of five were calculated for the targeted designed compounds (**5a–r**) (Table 1) using online Osiris Property explorer and Molinspiration property calculation toolkit [37–39]. The solubility (clogS) of synthesized molecules were found in an acceptable range ( $<-4$ ). The lipophilicity-related clogP enumerating target-oriented drug-likeness profile, drug potency, pharmacokinetics, and toxicity analysis has been implicated for many years. Compounds having  $<5$  clogP value was considered as more favorable drug-likeness profile [40, 41]. Among the series, all the synthesized compounds were found with  $<4$  clogP value which suggests their applicability for oral route of administration. Additional physicochemical parameters such as Topological Polar Surface Area (TPSA) were also calculated to detect poorly membrane permeable compounds with less CNS bioavailability which is beneficial for selecting oral drug candidates. Compounds with TPSA values  $>60\text{ \AA}$  are commonly picked for oral drug molecules [42]. The TPSA values

of our compounds were found in the range of  $107.50\text{--}153.30\text{ \AA}$ , which fascinates additional structural optimization for the development of new molecules. The drug-likeness properties suggested that compounds having zero or negative values should not be deliberated as drug-like applicant. In peculiarity of all synthesized compounds impelling drug-likeness scores  $>0$ , all compounds except **5d**, **5h**, and **5q** showed maximum drug-likeness score in between 1.03 and 5.20 as depicted in Table 1. The aforesaid online prediction software helped in distinguishing a set of compounds suitable for pharmacological screening.

### PASS prediction

PASS (Prediction of Activity Spectra for Substances) identifies the potential biological activities of a compound on the basis of comparison of its chemical structure with a database of existing quantitative structure–activity relationships (2D QSAR) of over 250000 compounds demonstrating over 4000 types of biological activities together with pharmacologic effects, mechanism of action, harmful and adverse effects, interaction with catabolic enzymes and transporters, significance on sequence expressions, etc. [43, 44]. Keeping in view the features of XO inhibitors, PASS prediction of compounds was performed in order to eliminate the synthesized compounds with probability of activity values (Pa) less than 0.400 and the remaining compounds were selected for gout treatment (Pa–Pi  $>0.4$ ) (Table 1). All the synthesized compounds (**5a–r**) exhibited the Pa value in the range of 0.466–0.532 and further performed *in vitro* screening also concentered the base of potency of the said compounds.

PASS prediction software also helped in recognition of those compounds which had more reliable results of docking studies. Low-docked compounds, with moreover lesser dock outcome or poorly docked poses, were designated as inactive.

### Molecular docking studies

Molecular docking studies of designed molecules for enzyme–inhibitor interactions was performed on XO (PDB entry 1N5X) using Glide XP Docking protocol in Schrodinger 9.4 [45–47]. Molecular docking variations includes van der Waals and electrostatic synergy between active site and ligand which is the basis of force field scoring. Chemical structures of the intended compounds were exposed to the active site of XO and results were compared with febuxostat. During docking analysis, validation for the accuracy of Glide docking program was established. The RMS deviation of Glide XP was calculated in between the most reasonable binding modes of febuxostat and co-crystallized structure febuxostat. The result of the control of Glide docking determined the finest orientation of the docked inhibitor, febuxostat to be close to that of the original orientation found in the crystal structure (Fig. 3). The MS deviation in-between the experimental conformation and the calculated docked conformation for febuxostat in XDH (1N5X) was  $0.63\text{ \AA}$ . The carboxylate group, which is the most tightly bound part in febuxostat was also present in our XO inhibitors and thus justified the similar binding pattern with amino acid. The oxygen atom of carboxylate group interacted

**Table 1.** *In silico* physicochemical properties for oral bioavailability and bioactivity of the test compounds evaluated utilizing computational predictive software.

Comp. ID	Compound type	Gout treatment		Dock score (kcal/mol)	XP score	cLogP	cLogS	MW	Rotatable bonds	Drug likeliness	Drug score	TPSA	Toxicity
		Pa	Pa–Pi										
5a	H	0.491	0.487	–12.202	–12.202	2.4	–3.35	262	3	3.44	0.85	107.50	NM, NT
5b	4-F	0.476	0.472	–12.249	–12.249	2.5	–3.67	280	3	2.97	0.81	107.50	NM, NT
5c	4-Cl	0.532	0.529	–12.424	–12.424	3.0	–4.09	296	3	5.20	0.77	107.50	NM, NT
5d	4-Br	0.475	0.471	–12.158	–12.158	3.12	–4.19	340	3	0.21	0.57	107.50	NM, NT
5e	4-CH <sub>3</sub>	0.529	0.526	–12.123	–12.123	2.74	–3.70	276	3	2.36	0.79	107.50	NM, NT
5f	4-OH	0.509	0.506	–12.017	–12.017	2.05	–3.06	278	3	3.79	0.87	127.70	NM, NT
5g	4-OCH <sub>3</sub>	0.468	0.464	–10.609	–10.609	2.33	–3.37	292	4	3.74	0.84	116.70	NM, NT
5h	4-NO <sub>2</sub>	0.458	0.454	–10.011	–10.011	1.48	–3.81	307	4	–8.62	0.42	153.30	SM, ST
5i	2-F	0.449	0.445	–10.014	–10.014	2.5	–3.67	280	3	2.01	0.78	107.50	NM, NT
5j	2-Cl	0.470	0.466	–9.504	–9.504	3.0	–4.09	296	3	3.77	0.76	107.50	NM, NT
5k	2-Br	0.459	0.455	–9.981	–9.981	3.12	–4.19	340	3	–0.30	0.53	107.50	NM, NT
5l	2-CH <sub>3</sub>	0.516	0.513	–10.601	–10.601	2.74	–3.70	276	3	3.19	0.81	107.50	NM, NT
5m	2-NO <sub>2</sub>	0.466	0.462	–10.431	–10.431	2.33	–3.37	292	4	3.74	0.84	116.70	SM, ST
5n	2-OCH <sub>3</sub>	0.510	0.507	–9.122	–9.122	2.05	–3.06	278	3	3.49	0.87	127.70	NM, NT
5o	2-OH	0.433	0.429	–12.321	–12.321	3.1	–4.40	314	3	1.03	0.64	107.50	NM, NT
5p	3-Cl, 4-F	0.487	0.483	–8.012	–8.012	3.0	–4.09	296	3	2.12	0.73	107.50	NM, NT
5q	3-Cl	0.475	0.471	–8.671	–8.671	3.12	–4.19	296	3	–1.09	0.46	107.50	NM, NT
5r	3-Br	0.449	0.445	–8.014	–8.014	2.5	–3.67	340	3	2.01	0.78	107.50	NM, NT
	Febuxostat	0.712	0.716	–13.809	–13.809	4.09	–4.27	316	4	–1.08	0.45	90.46	NM, NT

Pa, probability of being active; Pi, probability of being inactive; cLogP, lipophilicity; cLogS, water solubility; TPSA, topological polar surface area; NM, non-mutagenic; NC, non-carcinogenic; SM, slightly mutagenic; ST, slightly tumorigenic; NP, not predicted.

with side chain of guanidinium group of Arg880 with hydrogen bonds (2.01 Å) binding to the side chain, and hydroxyl with backbone amide of Thr1010 (2.51 Å). The N-3 of thiazole ring led to the formation of hydrogen bond between the thiazole nitrogen and carboxylate side chain of Glh802 (2.11 Å). Whole thiazole ring was rendered between two phenylalanine residues: Phe1009 (3.73 Å) and Phe914 (3.91 Å) with  $\pi$ - $\pi$  interactions; these interactions may support the stabilization of the binding patterns and also help in substrate recognition. A linker (–CONH–) introduced in between the substituted benzyl and thiazole rings, which confirmed the structural expansion of our lead molecules through hydrogen binding with amino acid Ser876. The substituted benzamide part of designed molecules was observed interleaved in between Leu648, Phe649, Phe1013, Lys771, and Pro1076 with Ser876-nitrile bond, which provided guidance for its alignment. Hydrophobic amino acids Leu648, Phe649, Phe1013, Lys771, Pro1076, Leu873, Leu1014, Val1011, Thr1010, Ser1008, Arg880, Ala1029, Ala1078, Glh802, Phe1009, and Phe914 appeared as a birdcage (Fig. 4). The designed compounds 5a–f mainly embraced hydrophobic interactions and attained excellent docking score of >–12 kcal/mol. The electron donating groups CH<sub>3</sub>, OH, OCH<sub>3</sub> and electron withdrawing group F, Cl, Br were appeared encircled by amino acids Leu648, Phe649,

Phe1013, Lys771, and Pro1076. Significant docking score of most active derivatives 5a–e was found to be –12.42, –12.24, –12.20, –12.15, –12.12 kcal/mol as depicted in Table 1. According to molecular docking analysis of 5a–e, we may suggest that the presence of large aromatic thiazole ring in the structure of 2-benzamido-4-methylthiazole-5-carboxylic acid derivatives gets fits in the active site of XO and favors their binding and inhibition toward XO (Figs. 3 and 4).

### Biological activity

*In vitro* XO inhibitory activity of compounds 5a–r was carried out spectrophotometrically by measuring uric acid levels at 295 nm (Table 2) [48–50]. Febuxostat was used as the reference drug. The synthesized 2-benzamido-4-methylthiazole-5-carboxylic acid derivatives demonstrated XO inhibitory activity, but less than that of febuxostat. The potency of the aforesaid compounds can be due to the presence of thiazole ring with free carboxylic acid. Assessment of their inhibitory effect led to an observation that the presence of electron withdrawing group leads to good XO inhibitory activity in comparison to electron donating group. The functional group located at *ortho* position slightly diminishes the XO activity with respect to functional group located at *para* position either in case of electron releasing group or electron

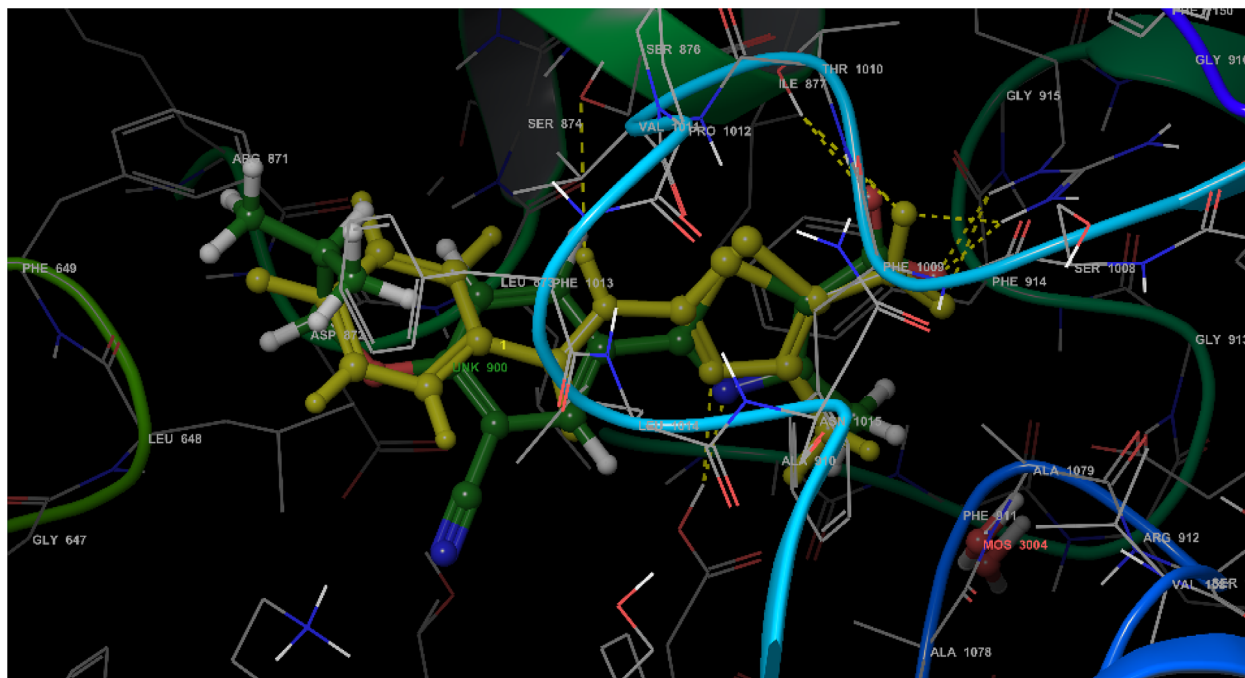


**Figure 3.** Top scored 3-dimensional (3D) diagrams representation showing hydrogen bonding interaction of compound **5b** (green) and febusostat (yellowish green) with active sites of enzyme xanthine oxidase (PDB ID: 1N5X) for XO inhibitory activity.

withdrawing group. The compounds **5h** and **5m** were not evaluated for XO inhibition due to their slight mutagenic effects as shown by *in silico* studies. Compounds **5i** ( $IC_{50} = 33.19 \mu\text{m}$ ), **5k** ( $IC_{50} = 59.69 \mu\text{m}$ ), **5n** ( $IC_{50} \geq 100 \mu\text{m}$ ), **5o**

( $IC_{50} = 47.25 \mu\text{m}$ ), **5q** ( $IC_{50} = 27.52 \mu\text{m}$ ), and **5r** ( $IC_{50} \geq 100 \mu\text{m}$ ) having substitution at *ortho* or *meta* position exhibited very low inhibitory activity. The compounds **5a** ( $IC_{50} = 14.57 \mu\text{m}$ ), **5e** ( $IC_{50} = 4.15 \mu\text{m}$ ), **5g** ( $IC_{50} = 12.67 \mu\text{m}$ ), **5j** ( $IC_{50} = 6.72 \mu\text{m}$ ), **5l**

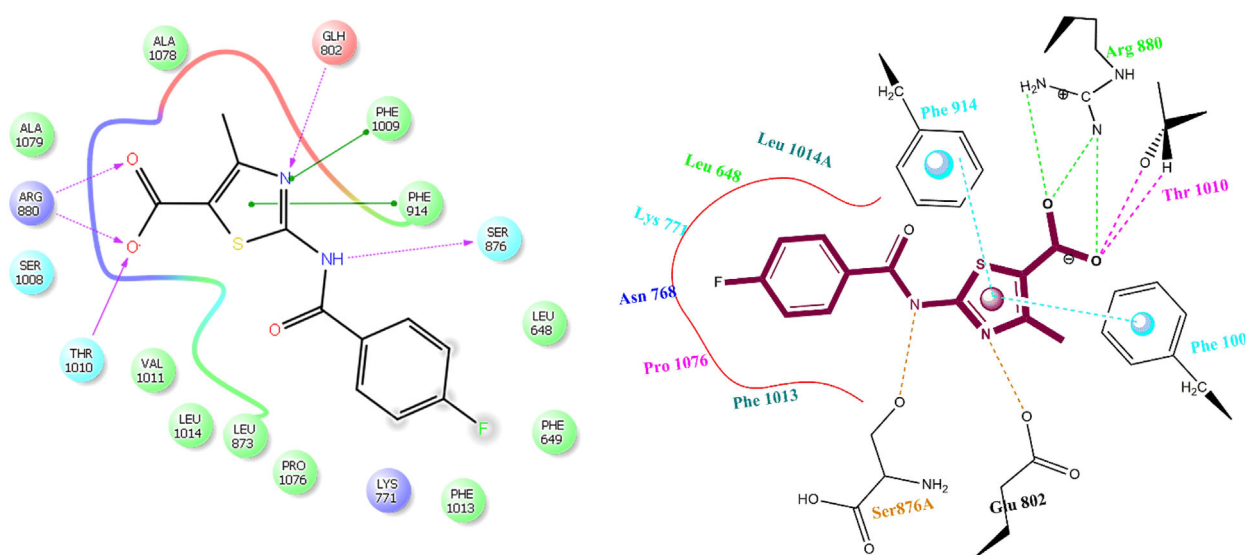


**Figure 4.** Top scored 2-dimensional (2D) diagrams showing hydrogen bonding interaction of compound **5b** with amino acids of active sites of enzyme xanthine oxidase (PDB ID: 1N5X).

**Table 2.** *In vitro* IC<sub>50</sub> values of XO inhibitory and free radical scavenging activities of derivatives.

Comp. ID	Compound	<i>In vitro</i> IC <sub>50</sub> (μM)	Free radical scavenging activity IC <sub>50</sub> (μM)	Uric acid inhibition (%) at 1 h, 10 mg/kg
5a	H	14.57 ± 0.09	29.18 ± 0.51	ND
5b	4-F	0.57 ± 0.34	23.21 ± 0.32	62
5c	4-Cl	0.91 ± 0.79	16.37 ± 0.11	53
5d	4-Br	72.01 ± 0.47	63.49 ± 0.17	ND
5e	4-CH <sub>3</sub>	4.15 ± 0.43	21.7 ± 0.73	35
5f	4-OH	28.37 ± 0.60	19.71 ± 0.35	ND
5g	4-OCH <sub>3</sub>	12.67 ± 0.59	28.93 ± 0.76	ND
5h	4-NO <sub>2</sub>	ND	ND	ND
5i	2-F	33.19 ± 0.21	>100	ND
5j	2-Cl	6.72 ± 0.37	61.7 ± 0.35	29
5k	2-Br	59.69 ± 0.41	>100	ND
5l	2-CH <sub>3</sub>	11.7 ± 0.04	31.21 ± 0.32	ND
5m	2-NO <sub>2</sub>	ND	ND	ND
5n	2-OCH <sub>3</sub>	>100	44.72 ± 0.47	ND
5o	2-OH	47.25 ± 0.43	22.26 ± 0.36	ND
5p	3-Cl, 4-F	4.97 ± 0.13	34.79 ± 0.81	41
5q	3-Cl	27.52 ± 0.07	58.12 ± 0.93	ND
5r	3-Br	>100	>100	ND
–	Febuxostat	0.01 ± 0.01	ND	73
–	Ascorbic acid	ND	12.7 ± 0.57	ND

ND, not determined; % inhibitor, calculated at 10 μM concentration (IC<sub>50</sub> value ± SD *n* = 3).

(IC<sub>50</sub> = 11.7 μm), and **5p** (IC<sub>50</sub> = 4.97 μm) exhibited significant XO inhibitory activity. Presence of halogen group at *para* position such as fluoro in compound **5b** (IC<sub>50</sub> = 0.57 μm) and chloro in compound **5c** (IC<sub>50</sub> = 0.91 μm) signify excellent XO inhibitory activity among the synthesized derivatives of this series. IC<sub>50</sub> values of all the compounds are depicted in Table 2. Enzyme kinetics study of most active inhibitor (**5b**) was performed. The Lineweaver–Burk plot (Fig. 5) analysis exhibited that compound **5b** is a mixed-type XO inhibitor. The graph pattern displays that it forms a mixed scenario of inhibition, the *K<sub>m</sub>*, *V<sub>max</sub>*, and slope all being affected by the inhibitor. A careful observation of Lineweaver–Burk plot represented that the intersecting lines on the graph converge to the left of the *y*-axis and above the *x*-axis which stipulated that the value of  $\alpha$  (a constant which defines that the affinity of the enzyme for substrate is affected by degree of inhibitor binding) is greater than 1, it was confirmed that the inhibitor is favorably binding with the free enzyme and not to the enzyme–substrate complex.

Antioxidant potential of 2-benzamido-4-methylthiazole-5-carboxylic acid derivatives was also evaluated using DPPH (1,1-diphenyl-2-picrylhydrazyl) assay [51]. 1,1-diphenyl-2-picrylhydrazyl (DPPH) is a stable free radical and accepts electron or hydrogen radical to become a stable diamagnetic molecule. Ascorbic acid was used as a reference compound. Derivatives **5d** (IC<sub>50</sub> = 63.49 μm), **5j** (IC<sub>50</sub> = 61.7 μm), **5k** (IC<sub>50</sub> ≥ 100 μm), **5l** (IC<sub>50</sub> = 31.21 μm), **5n** (IC<sub>50</sub> = 44.72 μm), **5p** (IC<sub>50</sub> = 34.79 μm), **5q** (IC<sub>50</sub> = 58.12 μm), and **5r** (IC<sub>50</sub> ≥ 100 μm) specified moderate free radical scavenging activity on the basis of their IC<sub>50</sub> values. Presence of electron or hydrogen radical releasing groups OCH<sub>3</sub>, OH, CH<sub>3</sub>, H in the structures of **5a**

(IC<sub>50</sub> = 29.12 μm), **5e** (IC<sub>50</sub> = 21.7 μm), **5f** (IC<sub>50</sub> = 19.71 μm), **5g** (IC<sub>50</sub> = 28.93 μm), and **5o** (IC<sub>50</sub> = 22.26 μm) may be responsible for reduction of DPPH free radical that imparts scavenging activity to them due to their electron donating activity. The compounds **5b** (IC<sub>50</sub> = 23.21 μm), **5c** (IC<sub>50</sub> = 16.37 μm), and **5f** (IC<sub>50</sub> = 19.71 μm) have significant DPPH free radical scavenging activity along with potent XO inhibitory activity, which is compared with standard, ascorbic acid. IC<sub>50</sub> values of the compounds of interest are depicted in Table 2.

#### Evaluation of the effect of xanthine oxidase inhibitors in hyperuricemic rat model assay

During evaluation of *in vitro* XO inhibitory study of 2-benzamido-4-methylthiazole-5-carboxylic acid derivatives (**5a–r**), compounds **5b**, **5c**, **5e**, **5j**, and **5p** were found to be most active among the series and were subjected to *in vivo* evaluation as anti-hyperuricemic agents in potassium oxonate-induced hyperuricemic rat model [52–54]. Dose of the compounds and standard was taken as potassium oxonate 300 mg/kg, febuxostat 10 mg/kg and test compounds as 10 and 20 mg/kg. *In vivo* study demonstrated that the compounds **5b**, **5c**, **5e**, **5j**, and **5p** exhibited 62, 53, 35, 29, and 41% of uric acid inhibition at 1 h, at a dose of 10 mg/kg. The compound **5b** is effective almost as the standard drug febuxostat and showed dose-dependent response graph (Fig. 6). The percentage uric acid inhibition at 1 h, at a dose of 10 mg/kg was found to be 62.00% whereas febuxostat showed 73.00% inhibition at a same dose level (Table 2). Hence the compound **5b** can be used for the management of gout and hyperuricemia because **5b** shows excellent uric acid inhibition along with free radical scavenging activity which

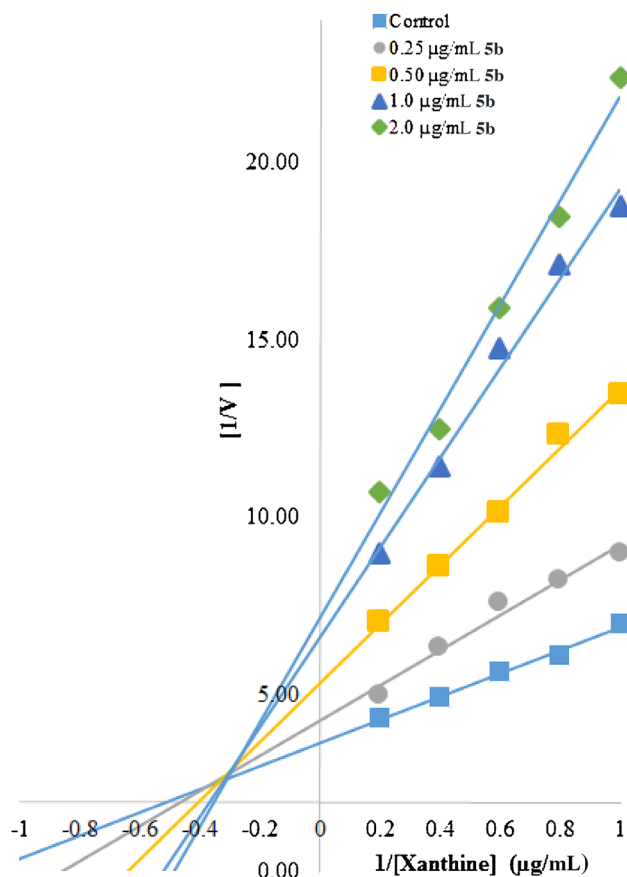


**Figure 5.** Lineweaver–Burk plot in the absence (control) and in the presence of inhibitor (**5b**) with xanthine as the substrate.

has not been reported in febuxostat. Therefore, **5b** could be used for further development of lead molecules.

## Conclusion

The synthesis of ethyl 2-benzamido-4-methylthiazole-5-carboxylate derivatives **5a–r** as febuxostat analogs was carried out successfully as per the scheme outlined in Scheme 1. All the structures of synthesized compounds were characterized by collective use of IR,  $^1\text{H}$  and  $^{13}\text{C}$  NMR, and mass spectroscopy. *In vitro* studies of these derivatives **5b** ( $\text{IC}_{50} = 0.57 \mu\text{m}$ ) and **5c** ( $\text{IC}_{50} = 0.91 \mu\text{m}$ ) signify excellent XO inhibitory activity among all the compounds in this series. Compounds **5b** ( $\text{IC}_{50} = 23.21 \mu\text{m}$ ), **5c** ( $\text{IC}_{50} = 16.37 \mu\text{m}$ ), and **5f** ( $\text{IC}_{50} = 19.71 \mu\text{m}$ ) also have a significant DPPH free radical scavenging activity along with potent XO inhibitory activity. Kinetic studies exhibited that **5b** acts as a mixed-type inhibitor. *In vivo* serum uric acid inhibition study on potassium oxonate-induced hyperuricemic rat model demonstrated that **5b** and **5c** displayed 62 and 53% of uric acid inhibition after 1 h at dose of 10 mg/kg.

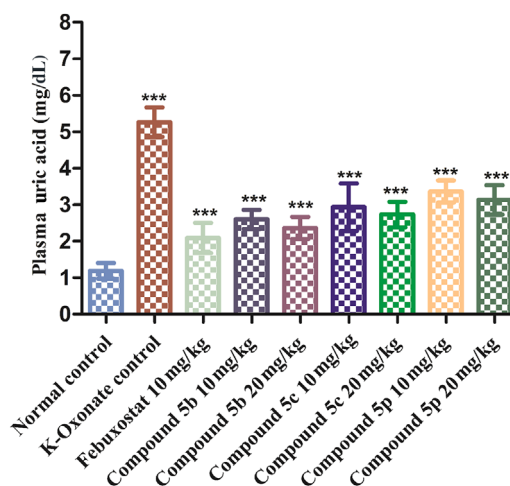


**Figure 6.** Serum uric acid concentration (mg/dL). Each value represents the mean  $\pm$  SEM ( $n = 5$ ). Bars with different letters are significantly different (\*\* $p < 0.01$ , \*\*\* $p < 0.001$ : ANOVA and post-Dunnet's test).

Overall it can be concluded that among the compounds in this series, compounds **5b** and **5c** demonstrated significant uric acid inhibition in both *in vitro* and *in vivo* studies. As compared with febuxostat, these compounds also revealed their *in vitro* DPPH free radical scavenging activity which has not yet been reported for standard. In conclusion, the overall study confirmed that compound **5b** may confer significant therapeutic benefits and a better safety profile over existing treatments for gout and hyperuricemia.

## Experimental

### Chemistry

#### General

All the solvents and reagent were obtained from reliable and authorized sources (S.D. Fi Chemicals, Sigma–Aldrich, Merck India, CDH Spectrochem, etc). All reactions were monitored by thin layer chromatography (TLC) using precoated silica gel G plates at 254 nm under UV lamp/iodine vapors using different solvent systems. Melting points were determined by the open capillary method with electric melting point apparatus and are uncorrected. Mass spectra (ESI-MS) were obtained by JEOL-AccuTOF JMS-T100LS mass spectrometer (JEOL USA, Inc., Peabody, MA, USA), and elemental analysis was performed on a Vario-EL III CHNOS. IR spectra were recorded on Bruker FT-IR spectrophotometer and  $^1\text{H}$  and  $^{13}\text{C}$  NMR spectra were recorded on Bruker DPX 300 MHz spectrophotometer (Bruker Bio Spin Corporation, Billerica, MA, USA) using  $\text{DMSO-}d_6$  or  $\text{CDCl}_3$  as solvent.

The NMR spectra and the InChI codes of the investigated compounds are provided as Supporting Information.

#### Synthesis of ethyl 2-amino-4-methyl-1,3-thiazole-5-carboxylate (**3**) [33–35]

To a mixture of anhydrous ethanol (100 mL) and thiourea (0.098 mol), ethyl-2-chloro acetoacetate (0.097 mol) was added drop-wise under constant stirring at room temperature. Once addition of ethyl-2-chloro acetoacetate is completed, reaction mixture was heated at 70–80°C for 15 min. Then reaction mass was cooled to room temperature and the solid precipitate was isolated, washed with 100 mL of cold ethanol and further washed with saturated sodium bicarbonate solution to obtain white solid which was finally dried under vacuum at 50°C for 8 h. Yield: 91%; white crystalline solid; m.p.: 170–172°C; IR (KBr  $\nu$  max): 3222, 3051, 1598, 1415, 1299, 698  $\text{cm}^{-1}$ ;  $^1\text{H}$  NMR (300 MHz, DMSO- $d_6$ );  $\delta$  1.36 (s, 3H, CH<sub>3</sub>), 2.62 (s, 3H, CH<sub>3</sub>), 4.32 (q, 2H, CH<sub>2</sub>CH<sub>3</sub>), 5.09 (bs, 2H, D<sub>2</sub>O exchangeable NH<sub>2</sub>); ESI-MS:  $m/z$  187.07 (M+H); Anal. calcd. for C<sub>7</sub>H<sub>10</sub>N<sub>2</sub>O<sub>2</sub>S: C, 45.15; H, 5.41; N, 15.04%. Found: C, 45.13; H, 5.42; N, 15.09%.

#### Synthesis of substituted ethyl 2-benzamido-4-methylthiazole-5-carboxylate (**4a–r**)

To a solution of substituted aromatic acids (0.001 mol) in 10 mL of dry pyridine, ethyl 2-amino-4-methyl-1,3-thiazole-5-carboxylate (**3**) (0.001 mol) was added and stirred at room temperature in flat bottom flask. The external temperature was maintained at 0–5°C. To the stirring saturated reaction mixture, 0.5 mL of POCl<sub>3</sub> was added dropwise and it was further stirred at room temperature till the completion of reaction. A solid precipitate was transferred into beaker containing crushed ice, and neutralized with glacial acetic acid, filtered and washed with water and dried, it was recrystallized with ethanol to give white solid products [34] (**4a–r**). The progress of the reaction and purity of the compound were checked by TLC, using toluene/ethyl acetate/formic acid (5:4:1) as mobile phase.

#### Ethyl 2-benzamido-4-methylthiazole-5-carboxylate (**4a**)

Yield: 63%; white crystalline solid; m.p.: 187–189°C; IR (KBr  $\nu$  max): 3273, 3083, 1733, 1665, 1489, 1376, 12009, 998  $\text{cm}^{-1}$ ;  $^1\text{H}$  NMR (300 MHz, DMSO- $d_6$ );  $\delta$  1.25 (d, 3H, CH<sub>3</sub>), 2.54 (s, 3H, CH<sub>3</sub>), 4.37 (q, 2H, CH<sub>2</sub>CH<sub>3</sub>), 7.28–8.01 (m, 5H, Ar-H), 12.10 (bs, 1H, D<sub>2</sub>O exchangeable CONH). Anal. calcd. for C<sub>14</sub>H<sub>14</sub>N<sub>2</sub>O<sub>3</sub>S: C, 57.92; H, 4.86; N, 9.65%. Found: C, 57.94; H, 4.85; N, 9.66%.

#### Synthesis of substituted ethyl 2-benzamido-4-methylthiazole-5-carboxylate (**5a–r**)

Substituted ethyl 2-benzamido-4-methylthiazole-5-carboxylate (**4a–r**) (0.075 mol) and potassium carbonate (0.3 mol) were added to a mixture of methanol/water (9:1) (20 mL). The solution was refluxed with stirring until the reaction was completed. The clear solution was cooled and neutralized with glacial acetic acid and stirred further for 25–30 min. Precipitate obtained was filtered, washed with water, dried and recrystallized with ethanol [33]. The progress of the reaction and purity of the compounds were checked by TLC, using benzene/acetone (8:2) as mobile phase.

#### 2-Benzamido-4-methylthiazole-5-carboxylic acid (**5a**)

Yield: 54%; white solid; m.p.: 133–135°C; IR (KBr  $\nu$  max): 3219, 3057, 1696, 1665, 1488, 1300, 1200, 813  $\text{cm}^{-1}$ ;  $^1\text{H}$  NMR (300 MHz, CDCl<sub>3</sub>);  $\delta$  2.26 (s, 3H, CH<sub>3</sub>), 6.82–7.86 (m, 5H, Ar-H), 12.22 (bs, 1H, D<sub>2</sub>O exchangeable CONH);  $^{13}\text{C}$  NMR (75 MHz, CDCl<sub>3</sub>); 17.86 (thiazole-CH<sub>3</sub>), 128.31, 128.91, 129.13, 129.26, 145.86, 156.54, 158.70, 163.54 (CONH), 167.70 (C=O); ESI-MS:  $m/z$  263.01 (M+H). Anal. calcd. for C<sub>12</sub>H<sub>10</sub>N<sub>2</sub>O<sub>3</sub>S: C, 54.95; H, 3.84; N, 10.68%. Found: C, 54.93; H, 3.85; N, 10.70%.

#### 2-(4-Fluorobenzamido)-4-methylthiazole-5-carboxylic acid (**5b**)

Yield: 49%; light pink solid; m.p.: 156–58°C; IR (KBr  $\nu$  max): 3257, 3071, 1743, 1670, 1499, 1323, 1045, 772  $\text{cm}^{-1}$ ;  $^1\text{H}$  NMR (300 MHz, CDCl<sub>3</sub>);  $\delta$  3.42 (s, 3H, CH<sub>3</sub>), 8.10–8.15 (t, 2H, Ar-H), 8.67–8.72 (m, 2H, Ar-H), 10.52 (bs, 1H, COOH), 12.13 (bs, 1H, D<sub>2</sub>O exchangeable CONH);  $^{13}\text{C}$  NMR (75 MHz, CDCl<sub>3</sub>); 17.79 (thiazole-CH<sub>3</sub>), 128.20, 128.36, 128.94, 135.53, 147.38, 149.09, 152.80, 165.03 (CONH), 169.05 (C=O); ESI-MS:  $m/z$  282.01 (M+2). Anal. calcd. for C<sub>12</sub>H<sub>9</sub>FN<sub>2</sub>O<sub>3</sub>S: C, 51.42; H, 3.24; N, 9.99%. Found: C, 51.43; H, 3.25; N, 10.01%.

#### 2-(4-Chlorobenzamido)-4-methylthiazole-5-carboxylic acid (**5c**)

Yield: 49%; light pink solid; m.p.: 187–189°C; IR (KBr  $\nu$  max): 3263, 3039, 1729, 1656, 1554, 1423, 1179, 1023, 812  $\text{cm}^{-1}$ ;  $^1\text{H}$  NMR (300 MHz, CDCl<sub>3</sub>);  $\delta$  2.60 (s, 3H, CH<sub>3</sub>), 7.28 (d, 2H,  $J=7.80$  Hz, Ar-H), 8.01 (d, 2H,  $J=8.10$  Hz, Ar-H), 12.11 (bs, 1H, D<sub>2</sub>O exchangeable CONH);  $^{13}\text{C}$  NMR (75 MHz, CDCl<sub>3</sub>); 17.07 (thiazole-CH<sub>3</sub>), 127.33, 128.78, 129.66, 144.13, 156.79, 160.34, 163.95 (CONH), 165.88 (C=O); ESI-MS:  $m/z$  297.13 (M+1). Anal. calcd. for C<sub>12</sub>H<sub>9</sub>ClN<sub>2</sub>O<sub>3</sub>S: C, 48.57; H, 3.06; N, 9.44%. Found: C, 48.58; H, 3.07; N, 9.42%.

#### 2-(4-Bromobenzamido)-4-methylthiazole-5-carboxylic acid (**5d**)

Yield: 53%; light yellow solid; m.p.: 201–203°C; IR (KBr  $\nu$  max): 3294, 3071, 1734, 1650, 1558, 1473, 1041, 679  $\text{cm}^{-1}$ ;  $^1\text{H}$  NMR (300 MHz, CDCl<sub>3</sub>);  $\delta$  3.71 (s, 3H, CH<sub>3</sub>), 6.76 (d, 2H,  $J=8.10$  Hz, Ar-H), 7.85 (d, 2H,  $J=8.10$  Hz, Ar-H), 12.14 (bs, 1H, D<sub>2</sub>O exchangeable CONH);  $^{13}\text{C}$  NMR (75 MHz, CDCl<sub>3</sub>); 16.79 (thiazole-CH<sub>3</sub>), 127.98, 128.53, 129.73, 143.34, 156.75, 160.59, 163.82 (CONH), 167.31 (C=O); ESI-MS:  $m/z$  339.43 (M–H). Anal. calcd. for C<sub>12</sub>H<sub>9</sub>BrN<sub>2</sub>O<sub>3</sub>S: C, 42.24; H, 2.66; N, 8.21%. Found: C, 42.26; H, 2.67; N, 8.23%.

#### 4-Methyl-2-(4-methylbenzamido)thiazole-5-carboxylic acid (**5e**)

Yield: 42%; nature: white solid; m.p.: 153–154°C; IR (KBr  $\nu$  max): 3367, 3031, 1753, 1649, 1563, 1421, 1029  $\text{cm}^{-1}$ ;  $^1\text{H}$  NMR (300 MHz, CDCl<sub>3</sub>);  $\delta$  2.59 (s, 3H, CH<sub>3</sub>), 2.65 (s, 3H, Ar-CH<sub>3</sub>), 7.28 (d, 2H,  $J=7.80$  Hz, Ar-H), 7.91 (d, 2H,  $J=8.10$  Hz, Ar-H), 12.03 (bs, 1H, D<sub>2</sub>O exchangeable CONH);  $^{13}\text{C}$  NMR (75 MHz, CDCl<sub>3</sub>); 17.13 (thiazole-CH<sub>3</sub>), 21.50, 128.19, 128.94, 129.22, 143.38, 156.37, 160.80, 162.91 (CONH), 165.65 (C=O); ESI-MS:  $m/z$

277.04 (M+H). Anal. calcd. for  $C_{13}H_{12}N_2O_3S$ : C, 56.51; H, 4.38; N, 10.14%. Found: C, 56.52; H, 4.39; N, 10.15%.

**2-(4-Hydroxybenzamido)-4-methylthiazole-5-carboxylic acid (5f)**

Yield: 29%; creamy white solid; m.p.: 185–187°C; IR (KBr  $\nu$  max): 3322, 3143, 3056, 1731, 1653, 1578, 1454, 1029, 809  $cm^{-1}$ ;  $^1H$  NMR (300 MHz,  $CDCl_3$ );  $\delta$  2.43 (s, 3H,  $CH_3$ ), 6.67 (d, 2H,  $J=7.80$  Hz, Ar-H), 7.53 (d, 2H,  $J=8.10$  Hz, Ar-H), 9.47 (bs, 1H, Ar-OH), 11.79 (bs, 1H,  $D_2O$  exchangeable NH); ESI-MS:  $m/z$  279.09 (M+H). Anal. calcd. for  $C_{12}H_{10}N_2O_4S$ : C, 51.79; H, 3.62; N, 10.07%. Found: C, 51.80; H, 3.63; N, 10.09%.

**2-(4-Methoxybenzamido)-4-methylthiazole-5-carboxylic acid (5g)**

Yield: 47%; white solid; m.p.: 159–161°C; IR (KBr  $\nu$  max): 3329, 3097, 1701, 1678, 1573, 1447, 1029, 973  $cm^{-1}$ ;  $^1H$  NMR (300 MHz,  $CDCl_3$ );  $\delta$  2.51 (s, 3H,  $CH_3$ ), 3.88 (s, 3H, Ar-OCH<sub>3</sub>), 6.97 (d, 2H,  $J=6.90$  Hz, Ar-H), 7.87 (d, 2H,  $J=7.20$  Hz, Ar-H); 10.30 (bs, 1H, COOH), 11.80 (bs, 1H,  $D_2O$  exchangeable CONH);  $^{13}C$  NMR (75 MHz,  $CDCl_3$ ); 18.36 (thiazole- $CH_3$ ), 60.78 (Ar-OCH<sub>3</sub>), 128.36, 128.93, 129.12, 129.35, 130.03, 142.12, 152.80, 158.69, 162.62 (CONH), 169.07 (C=O); ESI-MS:  $m/z$  293.13 (M+H). Anal. calcd. for  $C_{13}H_{12}N_2O_4S$ : C, 53.42; H, 4.14; N, 9.58%. Found: C, 53.43; H, 4.15; N, 9.57%.

**4-Methyl-2-(4-nitrobenzamido)thiazole-5-carboxylic acid (5h)**

Yield: 41%; dark yellow solid; m.p.: 210–212°C; IR (KBr  $\nu$  max): 3387, 3101, 1751, 1654, 1532, 1477, 1029  $cm^{-1}$ ;  $^1H$  NMR (300 MHz,  $CDCl_3$ );  $\delta$  2.77 (s, 3H,  $CH_3$ ), 7.97 (d, 2H,  $J=6.90$  Hz, Ar-H), 8.32 (d, 2H,  $J=7.20$  Hz, Ar-H); 10.51 (bs, 1H, COOH), 12.15 (bs, 1H,  $D_2O$  exchangeable CONH); ESI-MS:  $m/z$  308.35 (M+H). Anal. calcd. for  $C_{12}H_9N_3O_5S$ : C, 46.90; H, 2.95; N, 13.67%. Found: C, 46.92; H, 2.94; N, 13.68%.

**2-(2-Fluorobenzamido)-4-methylthiazole-5-carboxylic acid (5i)**

Yield: 49%; light orange solid; m.p.: 171–173°C; IR (KBr  $\nu$  max): 3373, 3031, 1773, 1644, 1563, 1462, 1029, 912  $cm^{-1}$ ;  $^1H$  NMR (400 MHz,  $CDCl_3$ );  $\delta$  2.31 (s, 3H,  $CH_3$ ), 7.68–8.03 (m, 4H, Ar-H), 11.93 (bs, 1H,  $D_2O$  exchangeable CONH); ESI-MS:  $m/z$  282.07 (M+H). Anal. calcd. for  $C_{12}H_9FN_2O_3S$ : C, 51.42; H, 3.24; N, 9.99%. Found: C, 51.43; H, 3.25; N, 10.02%.

**2-(2-Chlorobenzamido)-4-methylthiazole-5-carboxylic acid (5j)**

Yield: 36%; creamy white solid; m.p.: 149–151°C; IR (KBr  $\nu$  max): 3362, 3037, 1763, 1673, 1591, 1413, 1029, 783  $cm^{-1}$ ;  $^1H$  NMR (300 MHz,  $CDCl_3$ );  $\delta$  2.32 (s, 3H,  $CH_3$ ), 7.44 (m, 3H, Ar-H), 7.86 (s, 1H,  $J=7.80$  Hz, Ar-H), 12.16 (bs, 1H,  $D_2O$  exchangeable CONH); ESI-MS:  $m/z$  298.05 (M+2). Anal. calcd. for  $C_{12}H_9ClN_2O_3S$ : C, 48.57; H, 3.06; N, 9.44%. Found: C, 48.55; H, 3.07; N, 9.46%.

**2-(2-Bromobenzamido)-4-methylthiazole-5-carboxylic acid (5k)**

Yield: 44%; light pink solid; m.p.: 137–139°C; IR (KBr  $\nu$  max): 3342, 3071, 1751, 1654, 1587, 1029, 667  $cm^{-1}$ ;  $^1H$  NMR (300 MHz,  $CDCl_3$ );  $\delta$  2.29 (s, 3H,  $CH_3$ ), 7.67–7.89 (m, 4H, Ar-H), 12.10 (bs, 1H,  $D_2O$  exchangeable CONH); ESI-MS:  $m/z$  341.17 (M+2). Anal. calcd. for  $C_{12}H_9BrN_2O_3S$ : C, 42.24; H, 2.66; N, 8.21%. Found: C, 42.25; H, 2.67; N, 8.23%.

**4-Methyl-2-(2-methylbenzamido)thiazole-5-carboxylic acid (5l)**

Yield: 39%; light orange solid; m.p.: 174–176°C; IR (KBr  $\nu$  max): 3274, 3051, 1771, 1679, 1551, 1422, 1027  $cm^{-1}$ ;  $^1H$  NMR (300 MHz,  $CDCl_3$ );  $\delta$  2.32 (s, 3H,  $CH_3$ ), 2.58 (s, 3H,  $CH_3$ ), 7.15 (m, 3H, Ar-H), 7.66 (s, 1H,  $J=8.40$  Hz, Ar-H), 9.92 (bs, 1H, COOH), 11.92 (bs, 1H,  $D_2O$  exchangeable CONH);  $^{13}C$  NMR (75 MHz,  $CDCl_3$ ); 18.53 (thiazole- $CH_3$ ), 20.58, 128.18, 128.32, 128.91, 129.12, 146.88, 150.76, 158.66, 162.76 (CONH), 168.66 (C=O); ESI-MS:  $m/z$  277.19 (M+2). Anal. calcd. for  $C_{13}H_{12}N_2O_3S$ : C, 56.51; H, 4.38; N, 10.14%. Found: C, 56.53; H, 4.39; N, 10.13%.

**4-Methyl-2-(2-nitrobenzamido)thiazole-5-carboxylic acid (5m)**

Yield: 43%; pale yellow solid; m.p.: 163–165°C; IR (KBr  $\nu$  max): 3312, 3047, 1732, 1661, 1582, 1426, 1376, 1029  $cm^{-1}$ ;  $^1H$  NMR (300 MHz,  $CDCl_3$ );  $\delta$  3.43 (s, 3H,  $CH_3$ ), 8.15–8.65 (m, 4H, Ar-H), 12.52 (bs, 1H,  $D_2O$  exchangeable CONH); ESI-MS:  $m/z$  308.82 (M+2). Anal. calcd. for  $C_{12}H_9N_3O_5S$ : C, 46.90; H, 2.95; N, 13.67%. Found: C, 46.91; H, 2.96; N, 13.69%.

**2-(2-Methoxybenzamido)-4-methylthiazole-5-carboxylic acid (5n)**

Yield: 33%; nature: white solid; m.p.: 141–143°C; IR (KBr  $\nu$  max): 3376, 3067, 1752, 1672, 1581, 1437, 1284, 1061  $cm^{-1}$ ;  $^1H$  NMR (300 MHz,  $CDCl_3$ );  $\delta$  2.43 (s, 3H,  $CH_3$ ), 3.69 (s, 3H,  $CH_3$ ), 6.90 (s, 1H,  $J=7.20$  Hz, Ar-H), 7.03 (s, 1H, Ar-H), 7.47 (d, 2H, Ar-H), 11.87 (bs, 1H,  $D_2O$  exchangeable NH); ESI-MS:  $m/z$  293.13 (M+2). Anal. calcd. for  $C_{13}H_{12}N_2O_4S$ : C, 53.42; H, 4.14; N, 9.58%. Found: C, 53.43; H, 4.13; N, 9.56%.

**2-(2-Hydroxybenzamido)-4-methylthiazole-5-carboxylic acid (5o)**

Yield: 37%; dark brown solid; m.p.: 196–198°C; IR (KBr  $\nu$  max): 3335, 3137, 3052, 1753, 1653, 1540, 1410, 1242, 1029  $cm^{-1}$ ;  $^1H$  NMR (300 MHz,  $CDCl_3$ );  $\delta$  2.41 (s, 3H,  $CH_3$ ), 7.01–7.56 (m, 4H, Ar-H), 8.97 (bs, 1H, OH), 11.87 (bs, 1H,  $D_2O$  exchangeable NH); ESI-MS:  $m/z$  279.21 (M+2). Anal. calcd. for  $C_{12}H_{10}N_2O_4S$ : C, 51.79; H, 3.62; N, 10.07%. Found: C, 51.77; H, 3.63; N, 10.06%.

**2-(3-Chloro-4-fluorobenzamido)-4-methylthiazole-5-carboxylic acid (5p)**

Yield: 47%; light pink solid; m.p.: 163–165°C; IR (KBr  $\nu$  max): 3389, 3278, 3007, 1742, 1649, 1561, 1432, 989, 734  $cm^{-1}$ ;  $^1H$  NMR (300 MHz,  $CDCl_3$ );  $\delta$  2.27 (s, 3H,  $CH_3$ ), 7.07 (s, 1H, Ar-H),

7.23 (s, 1H,  $J = 6.40$  Hz, Ar-H), 7.48 (s, 1H, Ar-H), 12.11 (bs, 1H, D<sub>2</sub>O exchangeable CONH); <sup>13</sup>C NMR (75 MHz, CDCl<sub>3</sub>); 17.23 (thiazole-CH<sub>3</sub>), 124.03, 127.19, 128.23, 128.72, 129.89, 148.59, 157.56, 158.63, 162.13 (CONH), 166.93 (CO); ESI-MS:  $m/z$  317.09 (M+2); Anal. calcd. for C<sub>12</sub>H<sub>8</sub>ClFN<sub>2</sub>O<sub>3</sub>S: 45.80; H, 2.56; N, 8.90%. Found: 45.82; H, 2.57; N, 8.91%.

#### 2-(3-Chlorobenzamido)-4-methylthiazole-5-carboxylic acid (**5q**)

Yield: 33%; light orange solid; m.p.: 169–171°C; IR (KBr  $\nu$  max): 3343, 3103, 1787, 1653, 1549, 1487, 1263, 1082, 771 cm<sup>-1</sup>; <sup>1</sup>H NMR (300 MHz, CDCl<sub>3</sub>);  $\delta$  2.28 (s, 3H, CH<sub>3</sub>), 6.20 (bs, 1H, D<sub>2</sub>O exchangeable NH), 7.08 (d, 1H, Ar-H), 7.21 (d, 1H, Ar-H), 7.49 (s, 1H, Ar-H); ESI-MS:  $m/z$  298.08 (M+2). Anal. calcd. for C<sub>12</sub>H<sub>9</sub>ClN<sub>2</sub>O<sub>3</sub>S: C, 48.57; H, 3.06; N, 9.44%. Found: C, 48.54; H, 3.07; N, 9.46%.

#### 2-(3-Bromobenzamido)-4-methylthiazole-5-carboxylic acid (**5r**)

Yield: 41%; light brown solid; m.p.: 182–184°C; IR (KBr  $\nu$  max): 3307, 2997, 1761, 1642, 1569, 1453, 1281, 1041, 673 cm<sup>-1</sup>; <sup>1</sup>H NMR (300 MHz, CDCl<sub>3</sub>);  $\delta$  2.48 (s, 3H, CH<sub>3</sub>), 7.08 (bs, 1H, D<sub>2</sub>O exchangeable NH), 8.13 (s, 1H, Ar-H), 8.16 (s, 1H, Ar-H), 8.78 (s, 1H, Ar-H); ESI-MS:  $m/z$  341.27 (M+2). Anal. calcd. for C<sub>12</sub>H<sub>9</sub>BrN<sub>2</sub>O<sub>3</sub>S: C, 42.24; H, 2.66; N, 8.21%. Found: C, 42.23; H, 2.65; N, 8.23%.

### In silico computational studies

#### Molecular docking studies

Molecular docking study was carried out using Glide XP Docking protocol in Schrodinger 9.4 [45–47]. Co-crystal structure of xanthine dehydrogenase (XDH) with febuxostat (PDB entry 1N5X; resolution 2.8 Å) was selected based on superior crystal structure parameters and compared with other XO or XDH structures. There was no difference seen in the binding sites and co-crystal structures of XO and XDH. The schematic ligand database is designed on the basis of previous literature and synthetic schemes utilized for the structure-based drug design (SBDD). Using LIGPREP module within Maestro BUILD, ligand was prepared by default setting. The tautomeric forms of ligands were generated at physiological pH (7.0 ± 2.0 pH) which includes *keto* and *enol* forms of ligands. Thirty conformations for each ligand were generated and lowest energy conformers were used for the docking analysis. Protein was prepared, optimized, and minimized by Protein Preparation Wizard using OPLS-2005 force field and the RMSD limit from the structure of 0.3 Å using the Impref module of impact 5.9. Bond orders were assigned, hydrogen atoms were added, formal charges were treated, and water molecules were deleted. Active site for docking was defined as a grid box of dimensions 25 × 25 × 25 Å<sup>3</sup> around the centroid of the ligand assuming that the ligands to be docked are of similar size as the co-crystallized ligand. Availability of crystal structure of human XO facilitated the use of structure-based drug designing strategies for the search of novel bioactive molecules. SBDD

strategies were based on rapid and perfect computational methods for the approximation of receptor-ligand binding affinities. Using Glide XP module, the docking of molecules was done with Epik state penalties for different ionizations and tautomeric states. XP docking works as more stringent scoring functions include terms for hydrophobic enclosure and desolvation penalties. Different docking poses of ligands were generated and analyzed for interpretation of final results.

#### In silico study for bioactivity and physicochemical properties

For development of XO inhibitors with enhanced pharmacological profile, the prediction of physicochemical properties are most emphasizing parameters. All the designed compounds were evaluated for their oral bioavailability, physicochemical properties, toxicity, and online pharmacological activity by utilizing these online softwares Osiris Property Explorer, Molinspiration, and PASS computational study. clogP, clogS, MW, NROTB, Lipinski's rule of five, drug likeness, and toxicity were calculated using online Molinspiration property calculation toolkit and online OSIRIS Property explorer. With the help of Osiris Property Explorer software, toxicities were predicted which indicated that the synthesized compounds would be free of mutagenicity, tumorigenicity, reproductive side effects and irritation. Potential biological activities of a compound based on 2D QSAR including drugs, drug-candidates, leads, and toxic compounds exhibiting biological activities including pharmacological effects, mechanism of action, toxic and adverse effects, interaction with metabolic enzymes and transporters, influence on gene expressions, etc. can be predicted by PASS online software [43, 44]. The PASS prediction software helped in fast recognition of a set of probable compounds having much more reliable results of docking. This above online prediction software helped in quickly identifying a set of probable compounds and is also useful for screening of compounds for pharmacological activities.

### Biology

#### Xanthine oxidase inhibitory activity

All the synthesized compounds were evaluated using bovine milk XO (grade 1, ammonium sulfate suspension, purchased by Sigma-Aldrich) for XO inhibition assay. For measuring uric acid formation at 293 nm at 25°C under aerobic condition, the UV-visible spectrophotometer (EI 2371) was used. The reaction mixture containing 1 mL xanthine (0.15 mM), 2.5 mL potassium phosphate buffer (50 mM, pH 7.4), and 0.5 mL of XO solution (0.405 U/mL) was incubated for 5 min at 25°C. Inhibition of XO activity by different inhibitors was calculated by following the decrease in the uric acid creation at 293 nm at 25°C. The blank was prepared without enzyme solution. Febuxostat was used as positive control. The enzyme was pre-incubated for 5 min with test compounds (dissolved in DMSO, 1% v/v), and the reaction started by the addition of xanthine. DMSO (1% v/v) did not interfere with the enzyme

activity. All the experiments were performed in triplicate and values were stated as mean of three experiments [48–50].

XO activity was expressed as percentage inhibition of XO as follows:

$$\text{XO Inhibition rate (\%)} = (A_C - A_S/A_C) \times 100$$

where  $A_S$  and  $A_C$  represent the absorbances of the test compound and control, respectively. The  $IC_{50}$  values, i.e., the  $\mu\text{g}$  concentration of inhibitor necessary for 50% inhibition, were determined by using GraphPad (Prism) software.

Four different concentrations of inhibitor **5b** were used for kinetic studies with varying concentration of xanthine (0.2–1.0  $\mu\text{g/mL}$ ) and fixed concentration of enzyme (0.0405 U/mL) in potassium phosphate buffer (50 mM, pH 7.4) [51].

#### DPPH free radical scavenging assay

The stable 2,2-diphenyl-1-picrylhydrazyl (DPPH) was used for the determination of free radical scavenging activity of synthesized compounds (**5a–r**) by Koleva et al. method [52]. Dissimilar concentrations of test compounds (6.25–100  $\mu\text{M}$ ) in methanol were added independently to an equal volume of 100  $\mu\text{M}$  methanolic solution of DPPH and the reaction mixture was kept at room temperature for 15 min. The absorbance of the reaction mixture was recorded at 515 nm using a UV visible spectrophotometer. The control sample contained DPPH and methanol excluding test compounds. Ascorbic acid was used as standard. % Free radical scavenging activity was calculated using the following formula:

$$\text{Free radical scavenging (\%)} = (A_C - A_S/A_C) \times 100$$

where C represents control and S represents sample reaction mixture as described above in the method. The concentration of test compounds having 50% radical scavenging activity ( $IC_{50}$ ) was calculated by using GraphPad (Prism) software.

#### In vivo efficacy: Animals

Animals were obtained from Central Animal House Facility, Jamia Hamdard (Hamdard University), New Delhi-110062. Registration number and date of registration is 173/CPCSEA, 28 Jan, 2000. All the experimental protocols were carried out with the permission from Institutional Animal Ethics Committee (IAEC) and Committee for the Purpose of Control and Supervision on Experiments on Animals (CPCSEA), Government of India, application no. 1136.

#### In vivo efficacy: Potassium oxonate-induced hyperuricemic rat-model assay

The compounds showing significant *in vitro* XO inhibitory activity in comparison to the standard drug febuxostat were further evaluated by *in vivo* animal activity using potassium oxonate-induced hyperuricemic rat-model assay [52–54]. Overnight fasted Wistar rats of body weight 180–200 g, were grouped according to serum uric acid levels and then treated with potassium oxonate (300 mg/kg) intraperitoneally to induce hyperuricemia. One hour after potassium oxonate

administration, rats were treated with selected test compounds dissolved in a solution of polyethylene glycol 400 and ethanol (2:1) which were orally administered as 10 mg and 20 mg/kg, po, and standard (febuxostat 10 mg/kg, po) and after the time period of 1 h, blood was collected. Serum was obtained by allowing the blood sample to settle for 1 h at room temperature and after centrifugation (Sigma 3K-30) at 4000 rpm for 20 min. Serum uric acid levels were measured spectrophotometrically at 550 nm (at 25°C) using an auto analyzer (AUTOSPAN Liquid Gold Uric Acid Kit, Span diagnostic Ltd., Surat, India) in HAH Centenary Hospital, Jamia Hamdard New Delhi.

#### Statistical analysis

GraphPad Prism ver. 5.0 (GraphPad Software, San Diego, CA) was used for statistical analysis and results are expressed as mean  $\pm$  SEM. Groups of data were equated with the analysis of variance (ANOVA) followed by Dunnett's *t*-test. The values  $p < 0.001$  and  $p < 0.01$  were considered for statistically significant.

*Authors are thankful to Department of Pharmaceutical Chemistry, Jamia Hamdard, New Delhi for providing necessary facilities. Thanks is also due to Jamia Hamdard, IIT Delhi and JNU, New Delhi for recording spectral data. One of the authors (Md. Rahmat Ali) is grateful to the UGC (Moulana Azad National Fellowship), New Delhi, India, for providing financial assistance.*

*The authors have declared no conflicts of interest.*

## References

- [1] E. Suresh, *Postgrad. Med. J.* **2005**, *81*, 572–579.
- [2] A. Shoji, H. Yamanaka, N. Kamatani, *Arthritis Rheum.* **2004**, *51*, 321–325.
- [3] J. U. Adams, *Nat. Biotech.* **2009**, *27*, 309.
- [4] P. Richette, T. Bardin, *Lancet* **2010**, *375*, 318–328.
- [5] Y. Shi, J. Evans, K. Rock, *Nature* **2003**, *425*, 516–522.
- [6] P. Pacher, A. Nivorozhkin, C. Szabo, *Pharmacol. Rev.* **2006**, *58*, 87–114.
- [7] I. Fridovich, *J. Biol. Chem.* **1970**, *245*, 4053–4057.
- [8] C. Paul, L. Ying, C. Mario, P. H. Jia, C. Kanyanga, V. P. Bart, P. Luc, J. V. Arnold, V. B. Dirk, *J. Nat. Prod.* **1998**, *61*, 71–76.
- [9] B. Halliwell, J. M. C. Gutteridge, C. E. Cross, *J. Lab. Clin. Med.* **1992**, *119*, 598–620.
- [10] A. Meneshian, G. B. Bulkley, *Microcirculation* **2002**, *9*, 161–175.
- [11] C. E. Berry, J. M. Hare, *J. Physiol.* **2004**, *555*, 589–606.
- [12] A. Boueiz, M. Damarla, P. M. Hassoun, *Am. J. Physiol. Lung. Cell. Mol. Physiol.* **2008**, *294*, L830–L840.
- [13] M. Houston, A. Estevez, P. Chumley, M. Aslan, S. Marklund, D. A. Parks, B. A. Freeman, *J. Biol. Chem.* **1999**, *274*, 4985–4994.

- [14] U. Landmesser, S. Spiekermann, S. Dikalov, H. Tatge, R. Wilke, C. Kohler, D. G. Harrison, B. Hornig, H. Drexler, *Circulation* **2002**, *10*, 3073–3078.
- [15] Z. Ungvari, S. A. Gupte, S. Rkai, F. A. Recchia, S. Batkai, P. Pacher, *Curr. Vasc. Pharmacol.* **2005**, *3*, 221–229.
- [16] M. C. Desco, M. Asensi, R. Marquez, J. Martinez-Valls, M. Vento, F. V. Pallardo, J. Sastre, J. Vina, *Diabetes* **2002**, *51*, 1118–1124.
- [17] R. Hille, *Eur. J. Inorg. Chem.* **2006**, *10*, 1913–1926.
- [18] F. Arellano, J. A. Sacristan, *Ann. Pharmacother.* **1993**, *27*, 337–343.
- [19] K. Okamoto, B. T. Eger, T. Nishino, S. Kondo, E. F. Pai, T. Nishino, *J. Biol. Chem.* **2003**, *278*, 1848–1855.
- [20] G. W. Smith, V. Wright, *Br. J. Clin. Pract.* **1987**, *41*, 710–711.
- [21] A. M. Youssef, E. G. Neel, E. B. Villanueva, M. S. White, I. M. El-Ashmawy, B. Patrick, A. Klegeris, A. S. Abd-El-Aziz, *Bioorg. Med. Chem.* **2010**, *18*, 5685–5696.
- [22] M. K. Reinders, T. L. Jansen, *Clin. Interv. Ageing* **2010**, *5*, 7–18.
- [23] S. Ishibuchi, H. Morimoto, T. Oe, T. Ikebe, H. Inoue, A. Fukunari, M. Kamezawa, I. Yamada, Y. Naka, *Bioorg. Med. Chem. Lett.* **2001**, *11*, 879–882.
- [24] “New Drugs FY”. (2013), Pharmaceuticals and Medical Devices Agency, Japan.
- [25] T. Sato, N. Ashizawa, K. Matsumoto, T. Iwanaga, H. Nakamura, T. Inoue, O. Nagata, *Bioorg. Med. Chem. Lett.* **2009**, *19*, 6225–6229.
- [26] Synthesis of Lesinurad, AstraZeneca’s potential blockbuster drug for gout. Published 24 February (2014).
- [27] M. R. Ali, S. Kumar, O. Afzal, N. Shalmali, M. Sharma, S. Bawa, *Chem. Biol. Drug Des.* **2016**, *87*, 508–516.
- [28] Q. Guan, Z. Cheng, X. Ma, L. Wang, D. Feng, Y. Cui, K. Bao, L. Wu, W. Zhang, *Eur. J. Med. Chem.* **2014**, *85*, 508–516.
- [29] R. Kumar, K. Darpan, S. Sharma, R. Singh, *Expert. Opin. Ther. Patents* **2011**, *21*, 1071–1108.
- [30] S. Wang, J. Yan, J. Wang, J. Chen, T. Zhang, Y. Zhao, M. Xue, *Eur. J. Med. Chem.* **2010**, *4*, 2663–2670.
- [31] J. U. Song, S. P. Choi, T. H. Kim, C. K. Jung, J. Y. Lee, S. H. Jung, G. T. Kim, *Bioorg. Med. Chem. Lett.* **2015**, *25*, 1254–1258.
- [32] S. Chen, T. Zhang, J. Wang, F. Wang, H. Niu, C. Wu, S. Wang, *Eur. J. Med. Chem.* **2015**, *103*, 343–353.
- [33] Process for the preparation of febuxostat and salts thereof, Patent No-WO2011/073617A1.
- [34] Aminothiazole derivatives as human stearylcoa desaturase inhibitors, Patent No-WO2007130075A1.
- [35] P. C. Mhaske, K. S. Vadgaonkar, R. P. Jadhav, V. D. Bobade, *J. Kor. Chem. Soc.* **2011**, *55*, 882–886.
- [36] A. G. N. Christian, C. A. G. N. Montalbetti, V. Falque, *Tetrahedron* **2005**, *61*, 10827–10852.
- [37] T. Hou, J. Wang, W. Zhang, X. Xu, *J. Chem. Inf. Model.* **2007**, *47*, 460–463.
- [38] Molinspiration software or free molecular property calculation services (2 screens). Available from URL: [www.molinspiration.com/cgi-bin/properties](http://www.molinspiration.com/cgi-bin/properties) (last accessed 11.02.16).
- [39] T. Sander, *Osiris Property Explorer*, **2001**. Available from URL: <http://www.organic-chemistry.org/prog/peo/> (last accessed 18.02.16).
- [40] N. A. Meanwell, *Chem. Res. Toxicol.* **2001**, *24*, 1420–1456.
- [41] A. Tarcsay, K. Nyiri, G. M. Keseru, *J. Med. Chem.* **2012**, *55*, 1252–1260.
- [42] A. L. Hopkins, G. M. Keserü, P. D. Leeson, D. C. Rees, C. H. Reynolds, *Nat. Rev. Drug Discov.* **2014**, *13*, 105–121.
- [43] A. Lagunin, A. Stepanchikova, D. Filimonov, V. Poroikov, *Bioinformatics* **2000**, *16*, 747–748.
- [44] PASS software free molecular property calculation services. Available from URL: <http://www.pharmaexpert.ru/passonline/predict.php> (last accessed 21.02.16).
- [45] Maestro. (2013) Version 9.4, Schrödinger, LLC, New York, NY.
- [46] J. P. Hughes, S. Rees, S. B. Kalindjian, K. L. Philpott, *Br. J. Pharmacol.* **2011**, *162*, 1239–1249.
- [47] C. A. Lipinski, F. Lombardo, B. W. Dominy, P. J. Feeney, *Adv. Drug Deliv. Rev.* **2001**, *46*, 3–26.
- [48] P. Valentao, E. Fernandes, F. Carvalho, P. B. Andrade, R. M. Seabra, M. L. Bastos, *J. Agric. Food Chem.* **2001**, *49*, 3476–3479.
- [49] S. D. Beedkar, C. N. Khobragade, S. S. Chobe, B. S. Dawane, O. S. Yemul, *Int. J. Biol. Macromol.* **2012**, *50*, 947–956.
- [50] L. D. Kong, X. Pan, R. X. Tan, C. H. Cheng, *Cell. Mol. Life. Sci.* **2000**, *57*, 500–505.
- [51] L. Costantino, G. Rastrelli, A. Albasini, *Int. J. Pharm.* **1992**, *86*, 17–23.
- [52] I. I. Koleva, T. A. Van-Beek, J. P. Linsen, A. de-Groot, L. N. Evstatieva, *Phytochem. Anal.* **2002**, *13*, 8–17.
- [53] Y. Osada, M. Tsuchimoto, H. Fukushima, K. Takahashi, S. Kondo, M. Hasegawa, K. Komoriya, *Eur. J. Pharmacol.* **1993**, *241*, 183–188.
- [54] L. Kuraka, T. Kalnovicova, B. Lia, P. Turanil, *Clin. Chem.* **1996**, *42*, 756–760.